Pressure-dependent ^{13}C chemical shifts in proteins: Origins and applications

David J. Wilton[1], Ryo Kitahara[2,3], Kazuyuki Akasaka[2,4] and Mike P. Williamson[1,*]

[1]D. J. Wilton, M. P. Williamson

Dept of Molecular Biology and Biotechnology, University of Sheffield, Firth Court, Western Bank, Sheffield S10 2TN, UK

[2]R. Kitahara, K. Akasaka

RIKEN SPring-8 Center, 1-1-1 Kouto, Sayo-cho, Sayo-gun, Hyogo 679-5148, Japan

[3]Current address: College of Pharmaceutical Sciences, Ritsumeikan University, 1-1-1 Noji-higashi, Kusatsu 525-8577, Japan

[4]Current address: Department of Biotechnological Science, School of Biology-Oriented Science and Technology, Kinki University, 930 Nishimitani, Kinokawa 649-6493, Japan

[*]**Corresponding author:** M P Williamson, tel +44 114 222 4224, fax +44 114 222 2800, email m.williamson@sheffield.ac.uk

Keywords: pressure, ^{13}C chemical shift, genetic algorithm, γ-gauche effect, compression

Character count of the entire text including spaces: 42117

Abstract. Pressure-dependent ^{13}C chemical shifts have been measured for aliphatic carbons in barnase and Protein G. Up to 200 MPa (2 kbar), most shift changes are linear, demonstrating pressure-independent compressibilities. CH_3, CH_2 and CH carbon shifts change on average by +0.23, -0.09 and -0.18 ppm respectively, due to a combination of bond shortening and changes in bond angles, the latter matching one explanation for the γ-gauche effect. In addition, there is a residue-specific component, arising from both local compression and conformational change. To assess the relative magnitudes of these effects, residue-specific shift changes for protein G were converted into structural restraints and used to calculate the change in structure with pressure, using a genetic algorithm to convert shift changes into dihedral angle restraints. The results demonstrate that residual $^{13}C\alpha$ shifts are dominated by dihedral angle changes and can be used to calculate structural change, whereas $^{13}C\beta$ shifts retain significant dependence on local compression, making them less useful as structural restraints.

Introduction

The application of hydrostatic pressure to protein solutions leads to changes in both structure and dynamics of the proteins, because pressure favors states with smaller partial molar volume. High pressure has only a small effect on internal energy, and is therefore a much less drastic perturbation than for example temperature (Akasaka 2006; Meersman and Dobson 2006). It is thus a powerful method for investigating protein structure and dynamics. Structural changes in several proteins have been determined as a result of pressure (Iwadate et al. 2001; Kitahara et al. 2005; Refaee et al. 2003; Williamson et al. 2003; Wilton et al. 2008b), and have allowed characterization of low-energy excited states and of protein compressibility, which in turn relates to volume fluctuations of the protein at ambient pressure. Using pressure it has been possible to characterize the initial stages of pressure denaturation (Kitahara and Akasaka 2003; Refaee et al. 2003; Wilton et al. 2008b), and it was demonstrated that slow concerted motions such as ring flips are slowed at high pressure, whereas more rapid motions such as those probed by backbone ^{15}N relaxation are unaffected (Li et al. 1999; Orekhov et al. 2000; Sareth et al. 2000).

One of the most useful and sensitive parameters for characterizing structural change has been chemical shift. ^{1}H shifts can be used to obtain detailed structural information (Refaee et al. 2003; Williamson et al. 2003; Wilton et al. 2008a; Wilton et al. 2008b), while ^{15}N shifts also provide structural information (Akasaka and Li 2001; Akasaka et al. 1999). So far, ^{13}C chemical shifts have not been investigated. They are however expected to be very useful, because there is a clear relationship between ^{13}Cα and ^{13}Cβ shifts and backbone dihedral angles (Iwadate et al. 1999; Spera and Bax 1991; Wishart and Sykes 1994), and therefore changes in ^{13}C shift should be useful for

describing changes in protein structure with pressure, for example pressure denaturation. We therefore present here studies on the pressure dependence of ^{13}C shifts, aimed at determining what information they carry and how this can be used to characterize structures at high pressure. Pressure-dependent chemical shifts also offer a unique way of detecting the effects of bond and orbital compression.

Materials and Methods

Staphylococcal protein G B1 domain was expressed as the double ^{13}C, ^{15}N-labeled form and purified as described (Tunnicliffe et al. 2005), while double labeled barnase was expressed and purified as described (Cioffi et al. 2009). Chemical shift assignments were taken from Tunnicliffe et al. (2005) and Korzhnev et al. (2001) respectively, and confirmed using standard triple resonance NMR experiments. All NMR measurements were carried out on a Bruker Biospin DRX-800 operating at 800 MHz for proton, using a quartz cell connected to a hand pump, as described (Kamatari et al. 2004). ^{13}C chemical shifts were measured using constant-time HSQC spectra with folding in the carbon dimension to increase resolution. Spectra were acquired at 3 MPa (rather than at atmospheric pressure, 0.1 MPa, to avoid the risk of getting small bubbles in the solution), and at 50, 100, 150 and 200 MPa. Data were processed using FELIX (Accelrys Inc., San Diego, CA), and peaks were picked into a database which was analyzed using Excel (Microsoft Corp, Seattle, WA).

Cα and Cβ chemical shifts were calculated from the protein structure using the relationships described (Iwadate et al. 1999). The 20 amino acids (minus histidine and

cyst(e)ine, for which there were not enough experimental data) are grouped into five groups ([trp, leu, met, phe, tyr], [glu, gln, lys, arg, asp, asn], [val, ile, thr, pro], [ala, ser] and [gly]). Each group has a different dependence of secondary chemical shift (ie experimental shift minus random coil shift) on the backbone dihedral angles φ and ψ, with different distributions for Cα and Cβ. In addition, the (φ, ψ) chemical shift surface is different depending on whether the carbonyl and amide nitrogen are hydrogen bonded, implying that there are four possible surfaces for each residue, with carbonyl or amide hydrogen bonded or not. A full prediction of conformation-dependent shift therefore requires a total of 20 (φ, ψ) chemical shift surfaces (16 for Cβ since there is no glycine Cβ surface). The XPLOR program, using the ^{13}C restraints implemented by Kuszewski et al. (1995), was therefore modified to include 20 surfaces, and is available on request. For the XPLOR calculations, the crystal structure 1pga (Gallagher et al. 1994) was refined using multiple molecular dynamics trajectories at 200 K in the absence of chemical shift restraints followed by averaging of the structures until it reached equilibrium, as described (Wilton et al. 2008b). Heavy atom masses were set to 100, and after an initial energy minimization, a dynamics trajectory was calculated at 200 K using 1000 steps of 1 fs followed by 6000 steps of 2 fs (for the direct shift restraints, only 2000 steps were necessary), followed by slow cooling over 20 stages to 0 K, each consisting of 50 steps of 0.5 fs, and a final energy minimization. For the direct shift restraints, a carbon shift force constant of 1250 kcal mol^{-1} ppm^{-2} was used, while the dihedral angle restraints followed standard protocols. Each calculation was repeated 50 times and the resultant structures were averaged.

The genetic algorithm (GA) used a population of 200 chromosomes. Each chromosome contains 168 'genes' (one for each backbone atom) which define the position of a backbone atom relative to its neighbors by using backbone dihedral angles. Mutation of the gene changes the position of one backbone atom whilst keeping the bond lengths to its neighbors unchanged. For the three-atom fragment *A*-*B*-*C*, mutation of the gene *B* moves atom *B* to a different location but keeps the distances r_{AB} and r_{BC} fixed: it therefore moves *B* on a circle defined by the intersection of two spheres with radii r_{AB} and r_{BC}. This will therefore change the two dihedral angles corresponding to rotations about the *AB* and *BC* bonds. Mutations produced a random change in dihedral angles in the range $\pm 20^{o}$. The GA was run using a crossover probability of 0.1, which was turned off after 200,000 iterations. A crossover means that the genes of residues 1 to *m* are combined with the genes of residues *m*+1 to *n*, where *n* is the number of residues. It was run for a total of 10^6 iterations, and each run was repeated a total of 10 times with different starting random seeds in order to check for good sampling of conformational space. At each iteration, the fitter chromosomes were selected for mutation/crossover to make daughters, using a random selection such that the fittest was picked 50% of the time, the second fittest 25% of the time, the third fittest 12.5%, etc. Similarly, unfit chromosomes were replaced by fitter ones on the same random basis but inverted such that the least fit is picked 50% of the time, the 2nd least fit 25% of the time, etc. If the iteration produced a fitter solution, this replaced the unfit chromosome.

The fitness function was based on the chemical shifts of Cα and Cβ, and compared the calculated shifts (based on the (φ, ψ) chemical shift surfaces) with the experimental shifts. If the calculated Cα and Cβ shifts for a particular residue are C_a and

C_b respectively, and the target experimental shifts are T_a and T_b, then the fitness for each residue is

$$F_a = \left|\frac{C_a - T_a}{T_a}\right| + 1, F_b = \left|\frac{C_b - T_b}{T_b}\right| + 1$$

and the calculated fitness is given by

$$F = 0.5\sum F_n = 0.5\sum \left(F_a + F_b\right)$$

where the summation runs over all residues. If the target shift is undefined, then F_i is set equal to 1 (i = a or b). In addition, penalties are applied for changes in φ or ψ of more than 15º from the starting value, and changes in ω of more than 5º from 180º. If the difference in φ or ψ is more than 15º, then

$$F_n' = F_n(1 + 0.2\{[\text{difference in angle}-15]/15\}^2)$$

and if the difference in ω is greater than 5º (ie if -175 < ω < 175), then

$$F_n' = F_n + 3(1-|\omega/180|)$$

Results and Discussion

^{13}C chemical shift changes

^{13}C chemical shifts were measured from CH HSQC spectra of staphylococcal protein G B1 domain and the H102A mutant of barnase (*Bacillus amyloliquefaciens* endoribonuclease) at 25 ºC, and at a range of pressures from 3 MPa (30 bar) up to 200 MPa in steps of 50 MPa (Fig. 1). For both proteins, the majority of chemical shift changes were linear with pressure (Fig. 2). In our previous studies of ^{1}H chemical shift

changes with pressure, we have shown that linear shift changes are due to a gradual linear compression of the structure, while non-linear changes indicate the presence of alternative states with lower partial molar volume, whose relative concentrations increase with pressure. Although such states are of great interest for uncovering details of pressure-induced unfolding, they are not the focus of this work, and we therefore extracted the initial linear shifts by fitting chemical shift changes to a second-order polynomial, and using the first-order coefficient as the linear gradient. Figure 2 demonstrates that there are a range of gradients. However, on closer inspection it is clear that pressure-induced shift changes fall into three distinct groups: methyl, methylene and methine protons have distinct chemical shift behavior, listed in Table 1. These three groups have significantly different shift changes as assessed by *t*-tests, and there was no significant dependence on secondary structure, nor on protein.

There are a number of possible explanations for this observation. There is a well characterized effect on ^{13}C shift of bond length, that has arisen in quantum-chemical calculations of nuclear shielding, because of the need to take into account rovibrational effects (Jameson 1977; Laws et al. 1993; Lazzeretti et al. 1987). It is consistently true that a shortening of the bond length to any heavy atom produces an increase in shielding, or in other words a decrease in the chemical shift (Jameson 1977). Laws et al. (1993) observed an effect of approximately 60 ppm/Å for Cα, depending to some extent on the atoms and bonds involved: the effect for valine Cα was 60 ppm/Å but the effect for alanine was 57 ppm/Å. The most buried carbon atom in amino acids is the Cα atom, which is therefore most likely to be dominated by this effect, if present. Proteins have a typical volume compressibility of approximately 0.5%/kbar (Gekko and Hasegawa 1986; Refaee et al.

2003; Williamson et al. 2003; Wilton et al. 2008b). However, in proteins, most of the compressibility comes from compression of cavities and hydrogen bonds, not covalent geometry. A better model for bond compression is therefore graphite or diamond, which have linear covalent bond compressibilities of 0.02% and 0.0055%/kbar respectively (Lynch and Drickamer 1966). Assuming that the shielding effect is additive for each heavy atom covalent bond, and that bonds to protein Cα have compressibilities somewhere between the sp^3 value of diamond and the sp^2 value of graphite, we may therefore expect an effect on Cα shifts of between approximately -0.1 and -0.05 ppm due to bond compression over 200 MPa. It therefore appears that a significant fraction of the chemical shift changed observed for Cα (and possibly other CH and CH_2) carbons arises from bond compression. This does of course not explain the deshielding seen for methyl carbons.

Throughout the 1960's and beyond, observations of ^{13}C chemical shifts in organic compounds consistently observed what is usually known as the γ-gauche effect, in which a ^{13}C shift is shielded by γ substituents when they are in a *gauche* arrangement, ie when they are in close 1-4 steric proximity to the carbon. The effect is also observed for other heavy nuclei. Furthermore, a β effect was also described, in which β substituents produce a deshielding. These are generally explained in a somewhat vague way as a steric effect (Wehrli and Wirthlin 1976), although it is clear that the effect is not simply a repulsion between hydrogen atoms (Barfield and Yamamura 1990; Seidman and Maciel 1977). Early calculations (Marshall and Pople 1960) concentrated on the effect of steric compression on orbital geometries, and suggested that van der Waals repulsions should in general be shielding until the interacting atoms become very close, at which point they

become deshielding. A number of subsequent calculations became more sophisticated, but retained the same basic explanation. A popular model proposed by Li and Chesnut (1985) suggested that the γ-gauche effect is a weakly attractive term, in which the proximity of neighboring atoms leads to an expansion of atomic orbitals and hence a small shielding, whereas the β-effect is a stronger deshielding caused by contraction of atomic orbitals due to the very close proximity of β substituents. If this effect is responsible for the pressure-dependent effects seen here, then we would expect to see a relationship between the number of β substituents and the shift change, since we would expect that the relatively uniform compression of the protein would affect all local geometries roughly equally. Such a correlation is indeed found, but this is primarily because methyl groups (which in general have few β substituents) have a markedly positive or deshielding shift change (Table 1). If methyl groups are removed from the analysis, there is no correlation. We therefore conclude that this explanation does not account well for the observed data. In particular, it does not account well for the clear relationship between shift change and number of attached protons. To some extent, this is also a relationship between shift change and position along the sidechain, since methyl groups are always at the end of a sidechain, whereas CH_2 are always in the 'middle' and the largest group of CH are Cα carbons, at the other end.

Another popular explanation of the γ-gauche effect is again that it is a steric effect, but arises from changes in bond angles due to steric compression (Gorenstein 1977; Lambert and Vagenas 1981). A change in bond angle implies a change in bonding orbital hybridization, and therefore a change in the shielding of the nucleus. This also explains changes in $^1J_{CH}$ coupling constants, which are suggested to have the same origin. A γ-

gauche substituent thus generally leads to an upfield shift change and a decrease in $^1J_{CH}$. By contrast, the effect of pressure on methyl groups is to cause a downfield shift (Table 1) and an increase in $^1J_{CH}$ (Jackowski et al. 2007). In other words, whereas a γ-gauche substituent leads to a reduction in bond angle, pressure tends to produce a 'splaying out' of methyl groups, and therefore changes in the opposite direction. This explanation accounts for the difference in pressure-dependent shift behavior between CH_3 and other carbons: the 'splaying out' is much greater for methyls not only because they have more protons but also because they are at the end of sidechains.

It therefore appears that a combination of bond shortening and bond angle effects best accounts for the observed shift changes. We note that of the popular explanations for the γ-gauche effect, our data strongly favor one based on bond angle changes.

Direct structure refinement against chemical shifts

The preceding arguments suggest that the pressure-induced ^{13}C chemical shift changes are due to a compressive effect that depends to some extent on the geometry of the protein. We would therefore expect that in addition to the average changes listed in Table 1, the shift change would show significant variation depending on the local geometry, particularly for the ends of sidechains. However, one might expect that the more 'internal' atoms would show a more uniform effect of pressure, if their shift changes are influenced more by bond compression and effects related to the γ-gauche effect, which should be approximately the same for all Cα carbons except glycine and probably proline.

In agreement with this expectation, we observe that the standard deviation for the shift change is greatest for methyl carbons and smallest for Cα (Table 1).

Our studies using ^{1}H shifts (Iwadate et al. 2001; Refaee et al. 2003; Williamson et al. 2003; Wilton et al. 2008b) have shown that there is a small but significant structural change in proteins on application of the pressures used here, RMS coordinate changes being approximately 0.2 Å, and RMS changes in backbone dihedral angles being approximately 5º, with a rather larger change in sidechain dihedral angles. Cα and Cβ shifts have a well-known dependence on backbone dihedral angle (Iwadate et al. 1999; Spera and Bax 1991; Wishart and Sykes 1994), and one would therefore expect that some of the Cα and Cβ shift changes should be due to changes in backbone dihedral angles, these having a significant contribution to the overall shift change in some cases.

We therefore took the measured shift change for Cα and Cβ carbons in protein G, subtracted the mean pressure-dependent shift as listed in Table 1, and investigated whether the residual shift changes contain any information about the dihedral angle changes. We have previously shown how the structure of protein G changes in response to pressure (Wilton et al. 2008b), so we have a high-pressure structure for comparison.

As a first attempt, we used the Cα and Cβ chemical shift changes directly as restraints. Although the relationship between Cα and Cβ backbone dihedral angles φ and ψ is clearly defined (Iwadate et al. 1999), there is significant standard deviation in the relationship, due to uncharacterized local structural effects. This implies that for any given amino acid the Cα and Cβ shifts cannot be calculated from the crystal structure to better than approximately 1.0 ppm RMS. Conversely, the use of ^{13}C shifts to calculate structure has an associated error in the predicted angles. For example, the popular

program TALOS has an average uncertainty of approximately 13° for φ and 12° for ψ (Cornilescu et al. 1999). Similar considerations apply to the programs SHIFTS (Xu and Case 2002), PROSHIFT (Meiler 2003), SHIFTX (Neal et al. 2003) and SPARTA (Shen and Bax 2007). This error is usually small enough to generate useful structural restraints. More recent applications of ^{13}C chemical shifts have combined structural predictions with molecular dynamics (Cavalli et al. 2007) or the structure prediction program ROSETTA (Shen et al. 2008) and obtained excellent results, with structures that match the more conventionally determined ones to within approximately 1 Å.

However, for this study, such methods do not have the accuracy necessary to calculate the sub-Å structural changes expected as a result of pressure. We reasoned therefore that calculation of a *change* in structure based on a *change* in chemical shift is a much more accurate calculation, as long as the structural change is small (which it is here), and is valid even if the absolute relationship between shift and structure has an associated error, because similar errors should apply to both the low- and high-pressure structures. We should therefore be able to use the change in shifts directly as restraints on the changes in backbone dihedral angles. We therefore took a high-resolution crystal structure of protein G, measured the φ and ψ angles for each residue, and calculated the slope of the (φ, ψ) shift map at this point. The change in shift was then applied as a restraint on φ and ψ within XPLOR, with an initial direction defined by the maximum slope, and magnitude of the force proportional to the shift change. Thus, the residue was effectively searching for the contour line in the (φ, ψ) map where the change in shift from the starting value matched the experimental value for Cα and Cβ simultaneously (Figure 3). Because the exact shape of the (φ, ψ) map depends on the amino acid residue type and

whether it has hydrogen bonds to the backbone, it was necessary to provide 20 different (φ, ψ) maps, which required some recoding of XPLOR.

This method was largely unsuccessful, as assessed by a number of measures. The target ^{13}C shifts were not very well met (mean error 0.07 ppm, compared to an initial pressure-induced change of 0.17 ppm: this should be compared to the values for ^{1}H calculations, which for protein G were 0.001 and 0.054 ppm respectively). The high-pressure structures fitted the measured ^{1}H chemical shift changes very badly. The RMS structure change was almost twice as large as found using ^{1}H shift restraints (0.4 Å compared to 0.2 Å), and some of the backbone dihedral angles changed by over 20º, which is much larger than any changes seen for the ^{1}H calculations, and seems unreasonably large in view of the relatively small structural changes seen as a result of pressure both by NMR (Kitahara et al. 2005; Refaee et al. 2003; Williamson et al. 2003; Wilton et al. 2008a; Wilton et al. 2008b) and by crystallography (Colloc'h et al. 2006; Girard et al. 2005; Urayama et al. 2002). Figure 4 shows the Cα pseudo-dihedral angle (ie, the dihedral angle formed by four successive Cα atoms) for the ^{13}C-based calculation compared to our earlier ^{1}H-based calculation. For ^{1}H the high-pressure structure was always very similar to the low-pressure structure, whereas the ^{13}C calculations showed a number of large deviations, particularly at the start of the α-helix (residues 22-26 in Figure 4). And finally, with ^{1}H restraints the high-pressure structure had as expected a smaller volume, with the helix moving closer to the sheet, and the edges of the sheet wrapping more around the helix, but with ^{13}C restraints there was no consistent change in structure and the overall volume was if anything larger.

There are a number of possible reasons for this lack of success, of which the main reason is most likely that there are many residues for which a simultaneous fit to the Cα and the Cβ restraint is not possible, ie the two contour lines shown in Figure 3 do not cross. The molecular dynamics search looks for the best possible match to both restraints, and in a number of cases this resulted in a best solution that had moved a long way in φ and/or ψ, to a physically unreasonable position. Changes in dihedral angles in one residue affect the direction of the backbone in adjacent residues, and so large errors propagate through the structure. In addition, we note that once a residue has got close to its target contours, there is no force to move it along a contour to search for a better global match to the restraints, and therefore there is no force to alter one residue 'sideways' along a (φ, ψ) contour to allow its neighbor to achieve a better fit.

For both these reasons we decided that rather than using the shifts directly as restraints, it would be better to calculate the optimum (φ, ψ) combinations represented by the chemical shifts first, and then restrain the structure to these dihedral angles.

Refinement against backbone dihedral angles

The aim of this calculation is to use the measured Cα and Cβ chemical shift changes to derive optimum target values for the backbone φ and ψ dihedral angles, and then use a molecular dynamics procedure to calculate a structure based on these target angles. We assume that the structure does not change much as a result of pressure, as discussed above. Several optimization methods could potentially be used to obtain the (φ, ψ) restraints, but in each case the aim is to find a combination of φ and ψ that (a) matches

the shift change well, (b) is close to the starting structure, and (c) does not perturb the local structure too much: subsequent (φ, ψ) pairs must allow the backbone to continue in roughly the original direction. Thus, a change in (φ, ψ) for one residue will in general require changes to dihedrals in residues either side.

The optimization method used here was a genetic algorithm (GA). A GA represents the parameters to be optimized as a number of 'chromosomes', and alters these by processes inspired by evolution. The fitness of the system that results from the parameters, or 'phenotype', is computed as a function of the chromosome set, and the aim of the GA is to arrive at the fittest system. This is usually done by starting with a population containing chromosomes of different fitness, selecting fit parent chromosome sets for mutation or crossover, and replacing unfit sets by fitter daughter ones. GAs have had a wide range of applications in multidimensional searching (Bayley et al. 1998; Jones et al. 1997).

The GA represented the structure of protein G using chromosomes composed of 'genes' describing backbone φ and ψ angles. In order to allow some flexibility, particularly for maintaining the backbone fold, the backbone ω angle was also allowed to vary, although only by a few degrees.

Having obtained a target set of dihedral angles, these were applied as restraints within a standard XPLOR molecular dynamics protocol. Application of restraints derived from Cα shifts alone produced structures that appear reasonable (Figure 5b). The overall structural changes were smaller than in the direct shift-based calculation and matched the target shifts better. The main structural changes seen previously in the ^{1}H-based calculations were that the α-helix moved closer to the β-sheet, and strand 2 of the sheet

showed an increase in curvature, wrapping itself more around the helix. Strand 3 also moved closer to the helix, while the N-terminus moved further away. All these effects appeared in the Cα-based calculation, which implies both that the shift parameters were consistent and reasonably accurate, and that the calculation method was successful. The changes caused by the Cα restraints were approximately half as large as those previously calculated using ^{1}H shift restraints. In the ^{1}H calculation the helix and sheet moved closer by approximately 0.18 Å, whereas in the ^{13}Cα calculation the distance was 0.11 Å. The increase in twist in strand 2 was also approximately half as big in the ^{13}Cα-based calculation. Structural changes for the other strands were similar. The ^{13}Cα calculation also showed a reduction in the moment of inertia of the protein in the helix-sheet direction, though again less than that seen for ^{1}H. By contrast to the direct shift refinements described in the previous section, the resultant structures have backbone dihedral angles almost entirely in the allowed regions of the Ramachandran plot, as determined using Procheck (Laskowski et al. 1996).

By contrast, structure calculations based on either Cβ shift changes alone or both Cα and Cβ shift changes together were much less successful, giving unreasonable structures with large structural changes, and in particular a highly bent and unwound helix (Figure 5c). On inspection of the (φ, ψ) restraints, it is clear that again the GA was only able to find solutions that required large changes in dihedral angles, particularly for the calculation based on simultaneous Cα and Cβ shifts, despite the imposition of a penalty for so doing.

We therefore conclude that pressure-dependent Cβ shifts are not suitable as restraints for structure calculations, whereas Cα shifts are. The most likely explanation

for this observation is that the residual Cβ shifts, after subtraction of the average pressure-dependent shift as described above, retain a significant shift contribution from local compressions, whereas most of the residual variation in Cα shifts is from the desired changes in the backbone dihedral angles. This is not surprising since the Cβ atoms are in general more exposed on the surface of the residue and therefore more likely to be influenced by neighboring atoms. This does of course imply that it may be possible to obtain some information about sidechain packing from the magnitude of the Cβ shift changes, but this is unlikely to be the best method for doing so. Cα shifts may have some application as structure restraints, although they are likely in addition to contain effects from local compression. They can therefore be used together with ^{1}H restraints.

The genetic algorithm-based optimization method used here could in principle be used for the complete structure calculation, not only for the optimization of target backbone dihedral angles. Some success has been obtained using a GA for NMR structure calculation (Bayley et al. 1998), but this application required energy minimization following the GA calculation, because a GA is not well suited to such procedures. It therefore is more efficient to use the GA only for the initial angle optimization.

In summary, we have shown that there is a general effect of hydrostatic pressure on ^{13}C chemical shifts, which is dependent on the number of attached protons, and is most easily rationalized as a general effect of bond shortening, together with pressure-induced changes in bond angles. The latter is compatible with one rationalization of the well-known γ-gauche effect, implying that this may be the best general explanation. The residual shift changes caused by pressure are dominated for ^{13}Cα by changes in backbone

structure, and can be used as restraints in calculating the change in structure produced by pressure, but the residual effects on $^{13}C\beta$ (and presumably other aliphatic carbons) are dominated by structure-specific shift changes arising from local bond and angle compression.

Acknowledgements

We thank Dr E. J. Gardner for advice on the GA, Jenny Tomlinson for preparing the protein G sample, and Dr Maya Pandya for preparing the barnase sample and assistance with NMR processing. We acknowledge funding from the Biotechnology and Biological Sciences Research Council (grant BB/D521230/1).

Table 1. Chemical shift changes from 3 to 200 MPa, for different groups of carbon atoms

	Cα (not Gly)	Other CH	All CH	CH_2	CH_3
Protein G	-0.15±0.14	-0.17±0.14	-0.16±0.14	-0.10±0.17	0.25±0.12
	(37)	(19)	(56)	(58)	(31)
Barnase	-0.20±0.13	-0.18±0.18	-0.18±0.16	-0.08±0.17	0.23±0.20
	(50)	(18)	(68)	(43)	(49)
Combined	-0.18±0.13	-0.18±0.16	-0.17±0.15	-0.09±0.17	0.24±0.18
	(87)	(37)	(124)	(101)	(80)

Figures in parentheses are the number of values used. Only 7 Gly Cα could be assigned and therefore no statistically significant results could be obtained.

References

Akasaka K, Li H, Yamada H, Li RH, Thoresen T, Woodward CK (1999) Pressure response of protein backbone structure. Pressure-induced amide ^{15}N chemical shifts in BPTI. Protein Sci. 8:1946-1953

Akasaka K, Li H (2001) Low-lying excited states of proteins revealed from nonlinear pressure shifts in ^{1}H and ^{15}N NMR. Biochemistry 40:8665-8671

Akasaka K (2006) Probing conformational fluctuation of proteins by pressure perturbation. Chem. Rev. 106:1814-1835

Barfield M, Yamamura SH (1990) Ab initio IGLO studies of the conformational dependencies of α–, β– and γ–substituent effects in the ^{13}C NMR spectra of aliphatic and alicyclic hydrocarbons. J. Am. Chem. Soc. 112:4747-4758

Bayley MJ, Jones G, Willett P, Williamson MP (1998) GENFOLD: A genetic algorithm for folding protein structures using NMR restraints. Protein Science 7:491-499

Cavalli A, Salvatella X, Dobson CM, Vendruscolo M (2007) Protein structure determination from NMR chemical shifts. Proc. Natl Acad. Sci. USA 104:9615-9620

Cioffi M, Hunter CA, Pandya M, Packer MJ, Williamson MP (2009) Use of quantitative ^{1}H NMR chemical shift changes for ligand docking into barnase. J. Biomol. NMR 43:11-19

Colloc'h N, Girard E, Dhaussy AC, Kahn R, Ascone I, Mezouar M, Fourme R (2006) High pressure macromolecular crystallography: The 140-MPa crystal structure at 2.3 Å resolution of urate oxidase, a 135-kDa tetrameric assembly. Biochim. Biophys. Acta 1764:391-397

Cornilescu G, Delaglio F, Bax A (1999) Protein backbone angle restraints from searching a database for chemical shift and sequence homology. Journal of Biomolecular Nmr 13:289-302

Gallagher T, Alexander P, Bryan P, Gilliland GL (1994) Two crystal structures of the B1 immunoglobulin-binding domain of streptococcal protein G and comparison with NMR. Biochemistry 33:4721-4729

Gekko K, Hasegawa Y (1986) Compressibility-structure relationship of globular proteins. Biochemistry 25:6563-6571

Girard E, Kahn R, Mezouar M, Dhaussy AC, Lin TW, Johnson JE, Fourme R (2005) The first crystal structure of a macromolecular assembly under high pressure: CpMV at 330 MPa. Biophys. J. 88:3562-3571

Gorenstein DG (1977) A generalized gauche NMR effect in ^{13}C, ^{19}F and ^{31}P chemical shifts and directly bonded coupling constants. Torsional angle and bond angle effects. J. Am. Chem. Soc. 99:2254-2258

Iwadate M, Asakura T, Williamson MP (1999) Cα and Cβ carbon-13 chemical shifts in proteins from an empirical database. J. Biomol. NMR 13:199-211

Iwadate M, Asakura T, Dubovskii PV, Yamada H, Akasaka K, Williamson MP (2001) Pressure-dependent changes in the structure of the melittin α-helix determined by NMR. J. Biomol. NMR 19:115-124

Jackowski K, Kubiszewski M, Wilczek M (2007) ^{13}C and ^{1}H nuclear magnetic shielding and spin-spin coupling constants of ^{13}C-enriched bromomethane in the gas phase. Chem. Phys. Lett. 440:176-179

Jameson CJ (1977) The isotope shift in NMR. J. Chem. Phys. 66:4983-4988

Jones G, Willett P, Glen RC, Leach AR, Taylor R (1997) Development and validation of a genetic algorithm for flexible docking. J. Mol. Biol. 267:727-748

Kamatari YO, Kitahara R, Yamada H, Yokoyama S, Akasaka K (2004) High-pressure NMR spectroscopy for characterizing folding intermediates and denatured states of proteins. Methods 34:133-143

Kitahara R, Akasaka K (2003) Close identity of a pressure-stabilized intermediate with a kinetic intermediate in protein folding. Proc. Natl Acad. Sci. USA 100:3167-3172

Kitahara R, Yokoyama S, Akasaka K (2005) NMR snapshots of a fluctuating protein structure: Ubiquitin at 30 bar-3 kbar. J. Mol. Biol. 347:277-285

Korzhnev DM, Bocharov EV, Zhuravlyova AV, Tischenko EV, Reibarkh MY, Ermolyuk YS, Schulga AA, Kirpichnikov MP, Billeter M, Arseniev AS (2001) ^{1}H, ^{13}C and ^{15}N resonance assignment for barnase. Appl. Magn. Reson. 21:195-201

Kuszewski J, Qin J, Gronenborn AM, Clore GM (1995) The impact of direct refinement against $^{13}C\alpha$ and $^{13}C\beta$ chemical shifts on protein structure determination by NMR. J. Magn. Reson. Ser. B 106:92-96

Lambert JB, Vagenas AR (1981) Dependence of the γ carbon-13 shielding effect on the dihedral angle. Org. Magn. Reson. 17:265-269

Laskowski RA, Rullmann JAC, MacArthur MW, Kaptein R, Thornton JM (1996) AQUA and PROCHECK-NMR: Programs for checking the quality of protein structures solved by NMR. J. Biomol. NMR 8:477-486

Laws DD, De Dios AC, Oldfield E (1993) NMR chemical shifts and structure refinement in proteins. J. Biomol. NMR 3:607-612

Lazzeretti P, Zanasi R, Sadlej AJ, Raynes WT (1987) Magnetizability and ^{13}C shielding surfaces for the methane molecule. Mol. Phys. 62:605-616

Li H, Yamada H, Akasaka K (1999) Effect of pressure on the tertiary structure and dynamics of folded basic pancreatic trypsin inhibitor. Biophys. J. 77:2801-2812

Li S, Chesnut DB (1985) Intramolecular van der Waals interactions and chemical shifts: A model for β- and γ-effects. Magn. Reson. Chem. 12:625-638

Lynch RW, Drickamer HG (1966) Effect of high pressure on the lattice parameters of diamond, graphite, and hexagonal boron nitride. J. Chem. Phys. 44:181-184

Marshall TW, Pople JA (1960) Nuclear magnetic shielding and diamagnetic susceptibility of interacting hydrogen atoms. Mol. Phys. 3:339-349

Meersman F, Dobson CM (2006) Probing the pressure-temperature stability of amyloid fibrils provides new insights into their molecular properties. Biochim. Biophys. Acta 1764:452-460

Meiler J (2003) PROSHIFT: Protein chemical shift prediction using artificial neural networks. J. Biomol. NMR 26:25-37

Neal S, Nip AM, Zhang H, Wishart DS (2003) Rapid and accurate calculation of protein ^{1}H, ^{13}C and ^{15}N chemical shifts. J. Biomol. NMR 26:215-240

Orekhov VY, Dubovskii PV, Yamada H, Akasaka K, Arseniev AS (2000) Pressure effect on the dynamics of an isolated alpha-helix studied by ^{15}N-^{1}H NMR relaxation. J. Biomol. NMR 17:257-263

Refaee M, Tezuka T, Akasaka K, Williamson MP (2003) Pressure-dependent changes in the solution structure of hen egg-white lysozyme. J. Mol. Biol. 327:857-865

Sareth S, Li H, Yamada H, Woodward CK, Akasaka K (2000) Rapid internal dynamics of BPTI is insensitive to pressure: ^{15}N spin relaxation at 2 kbar. FEBS Lett. 470:11-14

Seidman K, Maciel GE (1977) Proximity and conformational effects on ^{13}C chemical shifts at γ-position in hydrocarbons. J. Am. Chem. Soc. 99:659-671

Shen Y, Bax A (2007) Protein backbone chemical shifts predicted from searching a database for torsion angle and sequence homology. J. Biomol. NMR 38:289-302

Shen Y, Lange O, Delaglio F, Rossi P, Aramini JM, Liu GH, Eletsky A, Wu YB, Singarapu KK, Lemak A, Ignatchenko A, Arrowsmith CH, Szyperski T, Montelione GT, Baker D, Bax A (2008) Consistent blind protein structure generation from NMR chemical shift data. Proc. Natl Acad. Sci. USA 105:4685-4690

Spera S, Bax A (1991) Empirical correlation between protein backbone conformation and Cα and Cβ ^{13}C NMR chemical shifts. J. Am. Chem. Soc. 113:5490-5492

Tunnicliffe RB, Waby JL, Williams RJ, Williamson MP (2005) An experimental investigation of conformational fluctuations in proteins G and L. Structure 13:1677-1684

Urayama P, Phillips GN, Gruner SM (2002) Probing substates in sperm whale myoglobin using high-pressure crystallography. Structure 10:51-60

Williamson MP, Akasaka K, Refaee M (2003) The solution structure of bovine pancreatic trypsin inhibitor at high pressure. Protein Sci. 12:1971-1979

Wilton DJ, Ghosh M, Chary KVA, Akasaka K, Williamson MP (2008a) Structural change in a B-DNA helix with hydrostatic pressure. Nucleic Acids Res. 36:4032-4037

Wilton DJ, Tunnicliffe RB, Kamatari YO, Akasaka K, Williamson MP (2008b) Pressure-induced changes in the solution structure of the GB1 domain of protein G. Proteins: Struct. Funct. Bioinf. 71:1432-1440

Wishart DS, Sykes BD (1994) The ^{13}C Chemical Shift Index: a simple method for the identification of protein secondary structure using ^{13}C chemical shift data. J. Biomol. NMR 4:171-180

Xu XP, Case DA (2002) Probing multiple effects on ^{15}N, ^{13}Cα, ^{13}Cβ, and ^{13}C' chemical shifts in peptides using density functional theory. Biopolymers 65:408-423

Figure legends

Figure 1. Overlay of CH HSQC spectra of double labeled barnase H102A. The region of the spectrum is shown that contains methyl groups. Spectra are shown for 3, 50, 100, 150 and 200 MPa, going from blue to red. Residue numbers are labeled.

Figure 2. Pressure-dependent ^{13}C chemical shift changes in protein G, for a selection of methyl resonances between 21 and 21.5 ppm. Some signals fit well to a linear pressure dependence, while others require a second-order polynomial fit. For comparison, the pressure dependence for a CH carbon is also indicated, folded in from a different region.

Figure 3. Methodology for direct refinement against Cα and Cβ shifts. For each residue, the target Cα and Cβ shifts each represent a contour in (φ, ψ) space, given by the nearest values that match the change in shift with pressure. To match the combined Cα and Cβ shifts, the residue must find a location where both the Cα and Cβ values are satisfied, represented by the open circles. It initially moves in a direction given by the biggest slope in (φ, ψ) space (arrow).

Figure 4. Cα pseudo-dihedral angles (the dihedral angle formed by four successive Cα atoms) for low- and high-pressure structures of protein G calculated using direct ^{1}H and ^{13}C shift restraints.

Figure 5. Structural changes in protein G calculated from (a) ^{1}H shift changes, as described in Wilton et al. (2008b). The helix is compressed toward the sheet, and strand 2

of the sheet (the nearest strand in this orientation) becomes more twisted. The low pressure structure is shown in blue, and the high pressure structure in red. (b) Cα shifts, using (φ, ψ) restraints calculated using a genetic algorithm. Colors as in (a). (c) Cα and Cβ shifts combined, using (φ, ψ) restraints calculated using a genetic algorithm. Colors as in (a).

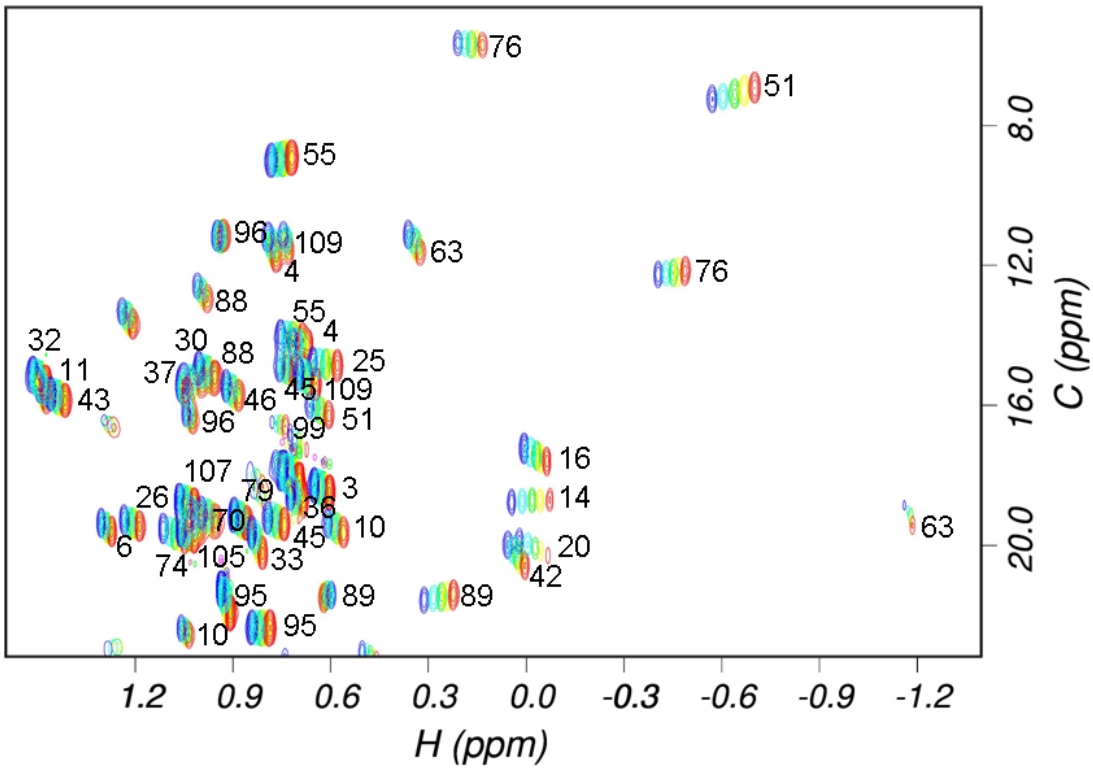
76
51
55
96
109
4
63
76
88
55
4
32
30
88
25
11
37
45
109
43
46
96
51
99
16
107
79
3
14
26
36
70
10
63
6
45
20
74
105
33
42
95
89
89
10
95
8.0
12.0
16.0
20.0
C (ppm)
1.2
0.9
0.6
0.3
0.0
-0.3
-0.6
-0.9
-1.2
H (ppm)

Fig. 1

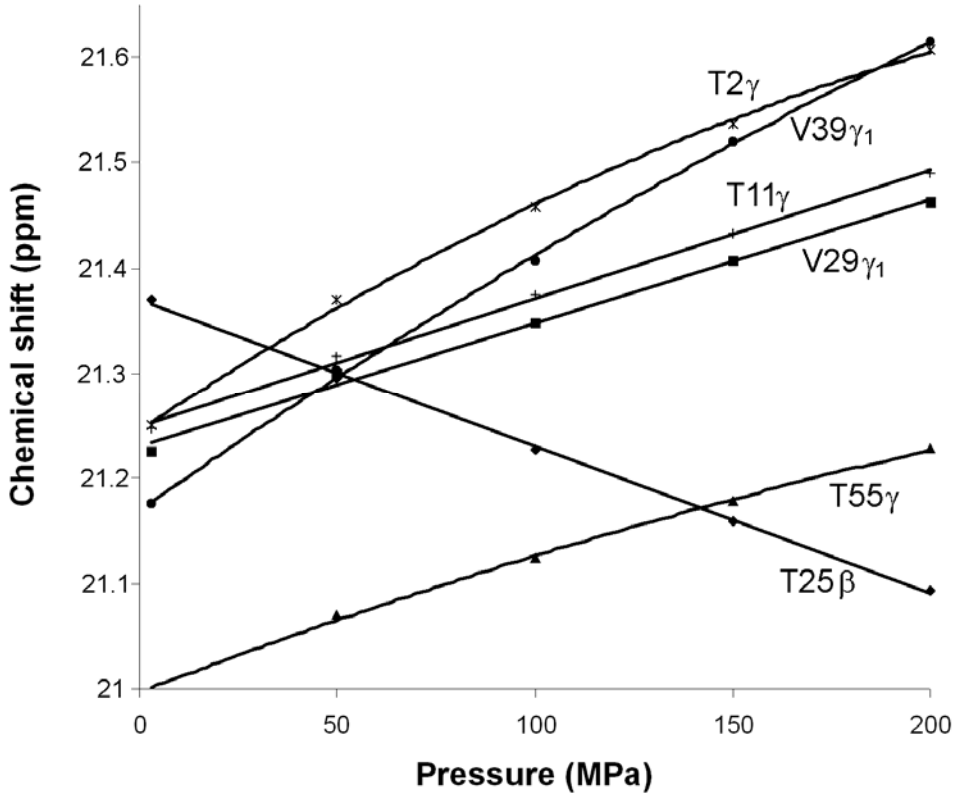
Chemical shift (ppm)
21.6
21.5
21.4
21.3
21.2
21.1
21
0
50
100
150
200
Pressure (MPa)
T2γ
V39γ1
T11γ
V29γ1
T55γ
T25β

Fig. 2

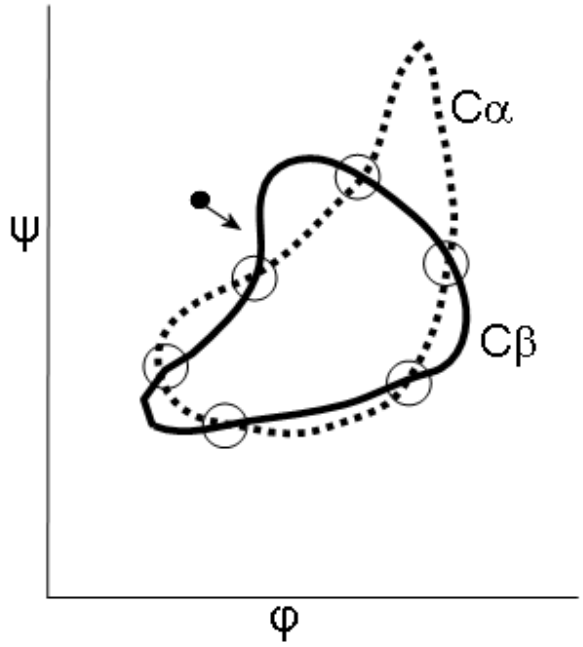
Cα
Cβ
Ψ
φ

Fig. 3

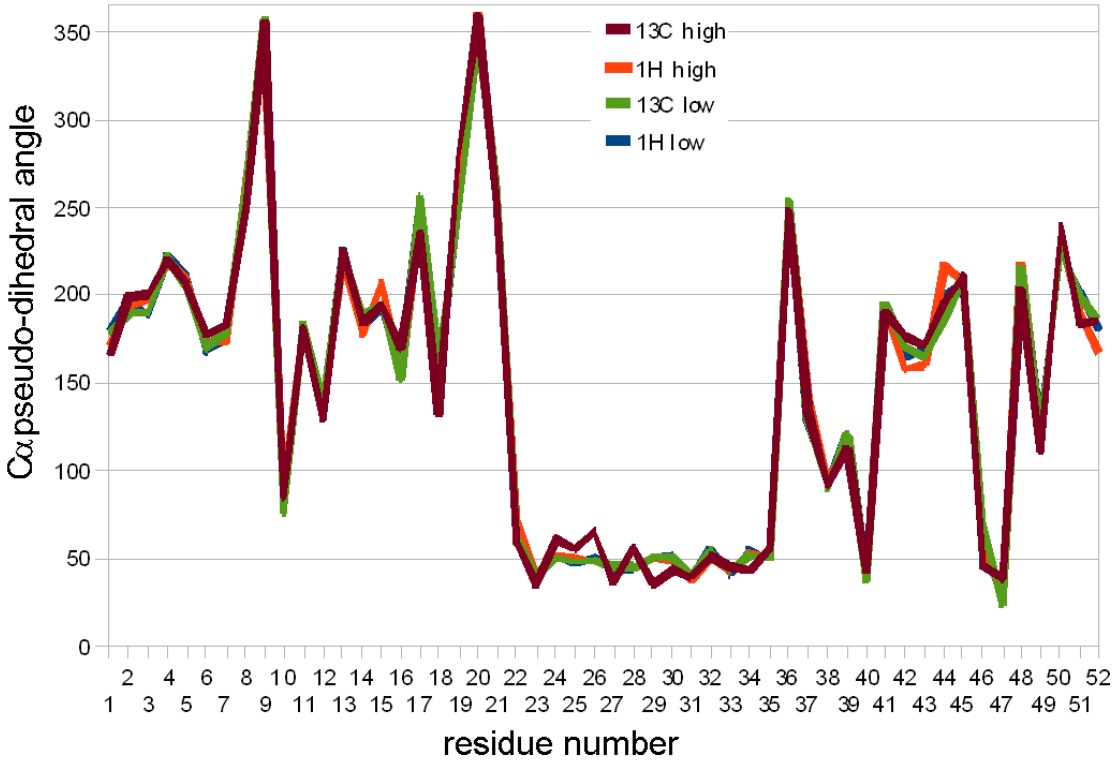
13C high
1H high
13C low
1H low
Cαpseudo-dihedral angle
0
50
100
150
200
250
300
350
1 2 3 4 5 6 7 8 9 10 11 12 13 14 15 16 17 18 19 20 21 22 23 24 25 26 27 28 29 30 31 32 33 34 35 36 37 38 39 40 41 42 43 44 45 46 47 48 49 50 51 52
residue number

Fig. 4

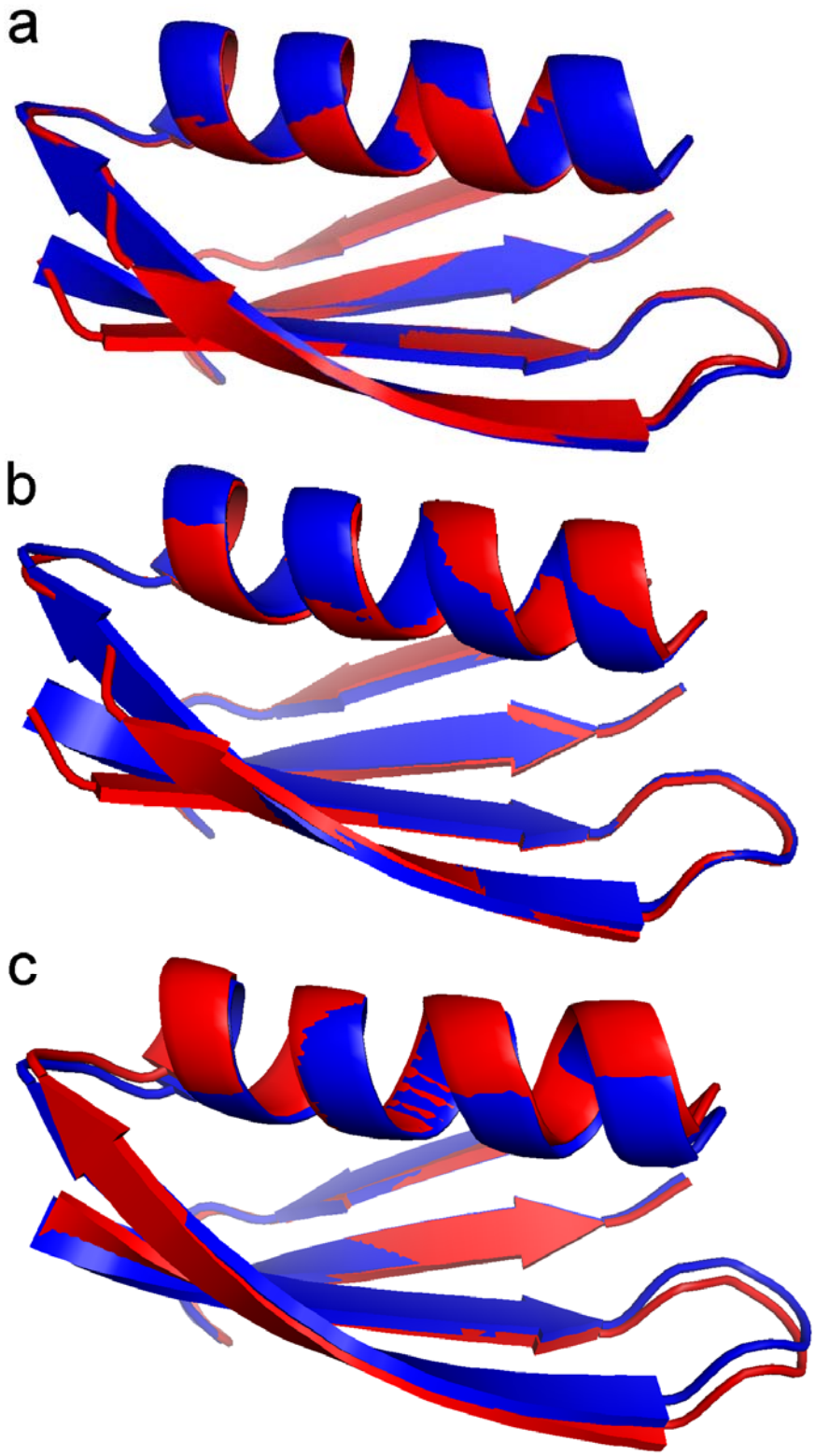

Fig. 5